

Visual detection of arginine, histidine and lysine using quercetin-functionalized gold nanoparticles

Karuna A. Rawat · Suresh Kumar Kailasa

Received: 16 March 2014 / Accepted: 14 May 2014 / Published online: 24 May 2014
© Springer-Verlag Wien 2014

Abstract We report on the use of quercetin-functionalized gold nanoparticles (QC-AuNPs) as a colorimetric probe for the amino acids arginine (Arg), histidine (His) and lysine (Lys). The method is based on the aggregation of the QC-AuNPs that is caused by these amino acids and leads to a visually detectable color change from red to blue. The absorption maxima shift from 525 nm to 702, 693, and 745 nm, respectively. Aggregations are confirmed by dynamic light scattering (DLS) and transmission electron microscopic techniques (TEM). The effects of the QC concentration, temperature and reaction time for the preparation of QC-Au NPs were tested. Other amino acids do not interfere. Under the optimal conditions, linear relationships exist between the absorption ratios at 702/525 nm (for Arg), 693/525 nm (for His), and 745/525 nm (for Lys) over the concentrations ranges from 2.5–1,250 μM (Arg) and 1–1,000 μM (His and Lys), respectively. The respective limits of detection are 0.04, 0.03, and 0.02 μM . The method provides a useful tool for the rapid visual and instrumental determination of the three amino acids.

Keywords Quercetin · AuNPs · Arginine · Histidine · Lysine · UV-visible spectrometry

Electronic supplementary material The online version of this article (doi:10.1007/s00604-014-1294-6) contains supplementary material, which is available to authorized users.

K. A. Rawat · S. K. Kailasa (✉)
Department of Chemistry, S. V. National Institute of Technology,
Surat 395007, India
e-mail: sureshkumarchem@gmail.com

S. K. Kailasa
e-mail: skk@ashd.svnit.ac.in

Introduction

The field of synthesis and studying of noble metal nanoparticles sensing properties is presently a very active research area in analytical chemistry. Since, many applications became possible by using metal NPs as probes for various analytes assays [1]. Meanwhile, the development of NPs-based approaches for the detection and screening of biomolecules is an important and highly active field of research because of the scientific and practical significance of miniaturized analytical tools. In the last decade, designing of metallic nano probes with higher efficacy depends on the controlled optical properties in the nanometer size range that can be of great utility in creating new smart nanomaterials for chemical and biomolecules readouts from complex samples [2–4]. In the era of nano probes, AuNPs are emerged as an integrated research area because of their unique tunable optical properties, which allows them to act as promising probes for signal readouts of various molecules at minimal volume of sample. For instance, AuNPs have been prepared by using various inorganic (NaBH_4) /organic reagents (sodium citrate, aspartic acid, tryptophan, hydroxylamine) and used as colorimetric probes for a wide variety of molecules [3–6]. Mostly, AuNPs can be produced by reducing chloroauric acid at high temperature with citrate as a reducing and stabilizing agent, which is described by Turkevich's group in 1951 [7]. Currently, many research groups have developed AuNPs-based colorimetric probes that involve the use of sodium borohydrate/citrate as reducing agents followed by their functionalization with various organic molecules for chemical and biomolecules sensing [3, 5, 8]. The colorimetric sensing ability of AuNPs is strongly dependent on their size and surface chemistry with controllable optical characteristics, which makes them as diverse probes for higher assay throughput. Since, the aggregation of AuNPs ($d > 3.5$ nm) induces interparticle surface plasmon coupling, resulting a red-shift in their SPR peak, which can be

observed by a visible color change from red to blue at nM concentrations.

It is well known that amino acids play a vital role in a variety of important cellular functions and have attracted attention because they are involved in numerous important functions in metabolism and cell regulations [9]. Importantly, three amino acids (Arg, His and Lys) are essentially needed for infants and human body. Traditionally, amino acids are quantified by using derivatization procedures coupled with various chromatographic techniques, which requires specific organic molecules for their derivatization and extremely time consuming. Thus, the development of NPs-based UV-visible spectrometric techniques has made it possible to detect underivatized amino acid samples rapidly without interference from other species in complex biological matrices at minimal volume of samples. Since, the size, shape and surface chemistry are very important and played key role in controlling physico-chemical and optical properties of AuNPs, which allow them to act as effective colorimetric probes for various target species [3]. Recently, Lee et al. modified AuNPs with triazole acetamide through Cu(I)-catalyzed single step reaction and used as a probe for detection of iodide ions [10]. Chansuvarn et al. developed a colorimetric method for detection of Hg^{2+} ion by using dithia-diaza capped AuNPs as a probe [11]. Similarly, Haghazari et al. reported the use of benzo crown-ether modified AuNPs as a probe for detection of Ag^+ ion in aqueous solution [12].

In this connection, several chemical synthetic routes have been described for the functionalization of AuNPs by using various organic molecules as capping agents and used as colorimetric probes for amino acids analysis. For instance, Qi et al. developed simple and sensitive colorimetric method for detection of cysteine by using carboxymethyl cellulose-functionalized AuNPs as nanoprobe [13]. Luo et al. demonstrated the application of ssDNA-stabilized AuNPs for simple and sensitive detection of cysteine [14]. Patel et al. reported the utility of *p*-sulfonatocalix[4]arene thiol modified AuNPs as colorimetric probes for detection of three amino acids (lysine, arginine and histidine) [15]. Chang and Tseng described the use of Tween 20-capped AuNPs as selective extracting and enriching probes for five aminothiols including amino acids (glutathione, γ -glutamylcysteine, cysteine, homocysteine, and cysteinylglycine) prior to their analysis by capillary electrophoresis [16]. Dong et al. reported the use of fluorescent conjugated polymer-stabilized AuNPs as fluorescent probes for detection of cysteine [17]. The detection of cysteine has been accomplished by using citrate capped AuNPs [18] and AuNPs conjugated with thermoresponsive copolymers [19] as colorimetric probes. George's group described a chemical route for the synthesis of AuNPs using cholesterol phenoxy hexanoate mesogens as a reducing and stabilizing agents [20]. Recently, Xie et al. developed dual detection method for cysteine by using silver nanoclusters as

colorimetric and fluorescent probes [21]. Furthermore, Jiang et al. reported a highly sensitive, rhodamine B-capped AuNPs-based dual readouts for sensing of organophosphorus and carbamate pesticides in complex solutions [22]. The same group developed azide- and alkyne- functionalized AuNPs as colorimetric probes for quantification of proteins in various sera and milk samples [23].

Even through these approaches successfully detected amino acids and small biomolecules with high selectivity and sensitivity, unfortunately these methods were involved extensive organic framework [2] or required two organic molecules (reducing and capping agent) [3, 5] for functionalization of AuNPs and their uses as molecular reorganization. Therefore, it is still a challenge to prepare controlled size AuNPs by using one organic reagent with multi-role (reducing and capping agent). Here we demonstrate the use of a simple one-pot synthetic approach for water-stabilized, monodisperse AuNPs that are coated with biomolecular recognition motifs on their surfaces. The QC not only reduces the chloroaurate but also acts as a capping agent on the surface of AuNPs, which results to control their size as well as color. Furthermore, there has been no report on the utilization of QC as a reducing and capping agent for preparation of AuNPs and their uses as sensor for analysis of amino acids in the literature. Therefore, we introduced QC as a novel reagent for one-pot synthesis of controlled size AuNPs and its application as a colorimetric probe for simultaneous sensing of three amino acids (Arg, His and Lys) in biological samples.

Experimental

Chemicals

Chloroauric acid ($\text{HAuCl}_4 \cdot x\text{H}_2\text{O}$), quercetin (2-(3,4-dihydroxyphenyl)-3,5,7-trihydroxy-4H-chromen-4-one), metal salts ($\text{Mg}(\text{NO}_3)_2 \cdot 6\text{H}_2\text{O}$, $\text{CaCl}_2 \cdot 2\text{H}_2\text{O}$, AlCl_3 , $\text{Na}_2\text{SO}_4 \cdot 10\text{H}_2\text{O}$, KNO_3 , $\text{Ba}(\text{NO}_3)_2 \cdot 4\text{H}_2\text{O}$) were obtained from Sigma-Aldrich, USA (www.sigmaaldrich.com). Amino acids (Arg, His, Lys, aspartic acid, cysteine, glutamic acid, methionine, phenyl alanine, serine, threonine, tyrosine and glucose, urea, uracil, guanine, guanosine, adenine and inosine) and NaOH were purchased from SRL Pvt. Ltd., India (www.srlchem.com). All chemicals were of analytical grade and used without further purification. Milli-Q-purified water was used for sample preparations.

Synthesis of QC-AuNPs

For a typical synthesis, a 10 mL of 1.0 mM HAuCl_4 solution was taken into a 50 mL round-bottom flask. To this, 0.5 mL of 2 mM QC freshly prepared in 10 mM of NaOH solution was added in a single purge. After 15 min, the light-yellow color of

solution was changed to red color, which confirms that the reduction of Au^{3+} to AuNPs. The AuNPs dispersed solution was stored at 4 °C prior to our analysis. In order to control the size and SPR band of AuNPs, we studied the various influencing parameters such as effect of QC concentration, temperature and time for formation of AuNPs with SPR peak at 525 nm and red color and these were measured by UV-visible absorption spectroscopy and digital camera.

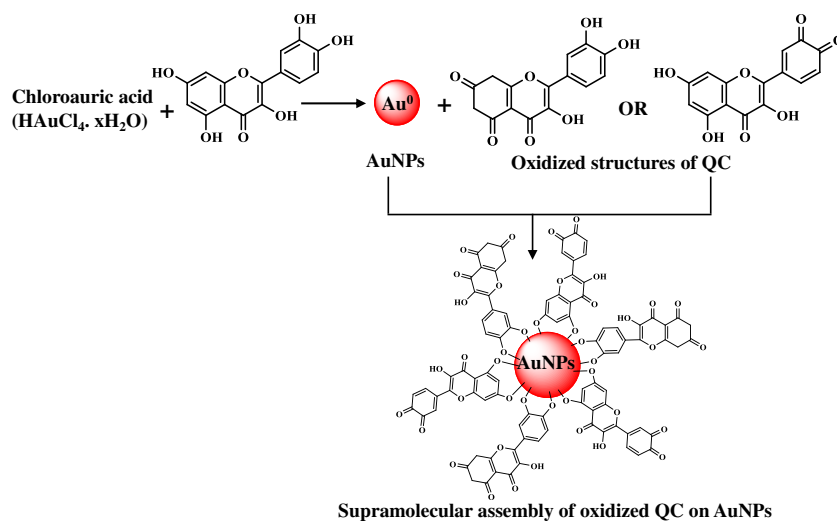
QC-AuNPs as a smart nano probe for arginine, histidine and lysine

We prepared stock solutions of Arg, His, and Lys (1.0 mM) in ultrapure water, and then added these amino acids (100 μL) solutions separately into 0.5 mL of 16.9 nM QC-AuNPs solution that contained phosphate-buffer (pH 5.0). The sample vials were vortexed for 2 min to facilitate induced QC-AuNPs aggregation with target species, resulting instantaneous color change from red to blue and UV-visible absorption spectra were measured. All UV-visible absorption spectra measurements were performed at room temperature under ambient conditions.

Analysis of histidine in urine samples using QC-AuNPs as a probe

We explore the potential applications of QC-AuNPs as colorimetric probes for analysis of His in urine samples. Urine samples were voluntarily collected from six healthy human (three females and three males). To determinate the concentration of His in a urine sample, the collected urine samples were diluted 50-folds using distilled water, to this, His (5, 15 and 25 μM) were spiked and added into QC-AuNPs solution that contained PBS buffer pH 5.0. The following steps were same as those described above in the quantification of standard solutions of three amino acids.

Scheme 1 Schematic diagram of proposed synthesis mechanism of QC-AuNPs



Instrumentations

The synthesized QC-AuNPs were characterized by Maya Pro 2,000 spectrophotometer (Ocean Optics, USA, www.oceanoptics.com). Fourier transform infrared (FT-IR) spectrometer (Perkin Elmer, FT-IR spectrum BX, Germany, www.perkinelmer.com). DLS (Zetasizer Nano ZS90, Malvern, UK, www.malvern.com) and transmission electron microscope (Phillips Tecnai, www.innovationsservices.philips.com).

Results and discussion

Effect of QC concentration

The effect of the concentration of QC on the preparation and functionalization of AuNPs was investigated. The QC-AuNPs are attributed to the reduction of Au^{3+} by QC as reducing and as a capping agent. The rationale behind the selection of QC is based on the fact that it exhibits both reducing and stabilizing groups, which allows functionalizing AuNPs in one-pot synthetic approach as shown in Scheme 1. However, it can be seen in the structure of QC, it has five phenolic groups, which can allow electron oxidation process to form quinone. In this sense, the concentration of QC is very important for preparation and functionalization of AuNPs. The formation of AuNPs by using different concentrations of QC (0.5–3 mM) was measured by UV-visible spectrometry. As shown in Fig. 1a, the absorbance and the position of the surface plasmon resonance (SPR) band of QC-AuNPs are strongly dependent on the concentration of QC. The corresponding absorption spectra and color of QC-AuNPs were clearly indicated that the QC-AuNPs exhibited broad SPR peak at 525 nm and the color intensity was gradually increased with increasing concentration of QC from 0.5 to 2.0 mM. It can be noticed that the SPR band at 525 nm become

more intense and sharp by using QC concentration at 2.0 mM. At higher concentrations of QC (2.5–3.0 mM), the SPR band became broad and further red-shifted (525–542 nm), resulting color change from red to blue, which is due to the formation of AuNPs clusters in the solution via hydrogen bonding, [24, 25], resulting broadening absorption band in the UV–visible spectra. Therefore, we selected 2.0 mM of QC as the best concentration for formation of QC-AuNPs with good SPR peak intensity and red monodispersion.

Effect of temperature and reaction time

In order to ensure whether temperature has any influence on the reduction rates of Au^{3+} ions, we recorded UV-visible absorption spectra of QC-AuNPs at different reaction temperatures from 0 to 100 °C. As shown in Fig. 1b, the intensity of SPR band at 528 nm became more and the peak is very sharp at room temperature. It was observed that the absorbance of QC-AuNPs was very poor and the SPR peak was broad at reaction temperatures 0, 50, 75 and 100 °C, respectively. We also observed that the color of QC-AuNPs solution was also changed from red to blue color at 50, 75 and 100 °C, which that confirms their size enlargement by hydrogen bond between QC-AuNPs. Based on the above results, we carried out QC-AuNPs synthesis at room temperature.

We also studied the effect of reaction time for the formation of QC-AuNPs with controlled size and red color by measuring UV-visible spectra at different reaction time intervals. As shown in Supporting Information of Fig. S1, the SPR peak intensity and color of QC-AuNPs solution were gradually increased with increasing reaction time up to 15 min, after that the absorption peak was slightly broad and intensity was following down. It is well know that interparticle spacing is decreasing with increasing reaction time, yielding slight red-shift and broad peak [26]. The SPR peak and color of QC-AuNPs as function of time indicates that there is a slight aggregation after 15 min reaction time. We believe that all Au^{3+} ions are completely reduced by QC at reaction time 15 min, after that AuNPs interparticle distances are gradually decreased, and yielded to change their SPR band, but color remains red.

Characterization of QC-AuNPs

FT-IR spectroscopy gave qualitative information about the chemical environment of QC before and after its oxidation in which the Au^{3+} ion are reduced to AuNPs. Supporting Information of Fig. S2 shows the FT-IR spectra of pure QC and QC-AuNPs. From FT-IR spectrum of pure QC, the peak appearing at 1,663 cm^{-1} was due to characteristic stretching vibration of C = O in QC, and the peak at 1,095 cm^{-1} was due to typical benzopyran group of QC. The peaks at 1,612, 1,518, 1,431 cm^{-1} are corresponding to the characteristics aromatic

–C = C- stretching in QC. Importantly, a strong peak at 3,370 cm^{-1} represented the stretching vibrations of phenolic –OH group in QC. However, stretching and vibrations peaks of QC were completely decreased or changed after reduction of Au^{3+} ion. For instance, the peak at 806 cm^{-1} arises from = C-H deformations of the benzene ring in QC. The phenolic -OH peaks shifted significantly to lower wave numbers at 3,783 cm^{-1} and their intensities were drastically decreased, which confirms the involvement of QC in reduction of Au^{3+} ion through polar OH groups. Similarly, a distinct spectral change in pure QC at 1,242 cm^{-1} and in QC-AuNPs at 1,249 cm^{-1} , which confirms that the phenolic C-O-H stretching red shift in QC-AuNPs due to molecular assembly on AuNPs. In addition, benzopyran group and cyclobenzene skeleton peaks are appearing in QC-AuNPs at 1,091 and 1,643, 1,518, 1,436 cm^{-1} , confirming the presence of QC molecules on the AuNPs surfaces. Therefore, QC was successfully acted as a reducing and capping agent for preparation of controlled size AuNPs with QC molecular assembly in step procedure.

Furthermore, we also calculated approximate average size of QC-AuNPs based on UV-visible spectra of QC-AuNPs, which is well described in the literature [27].

$$d = \exp\left(B_1 \frac{A_{spr}}{A_{450}} - B_2\right)$$

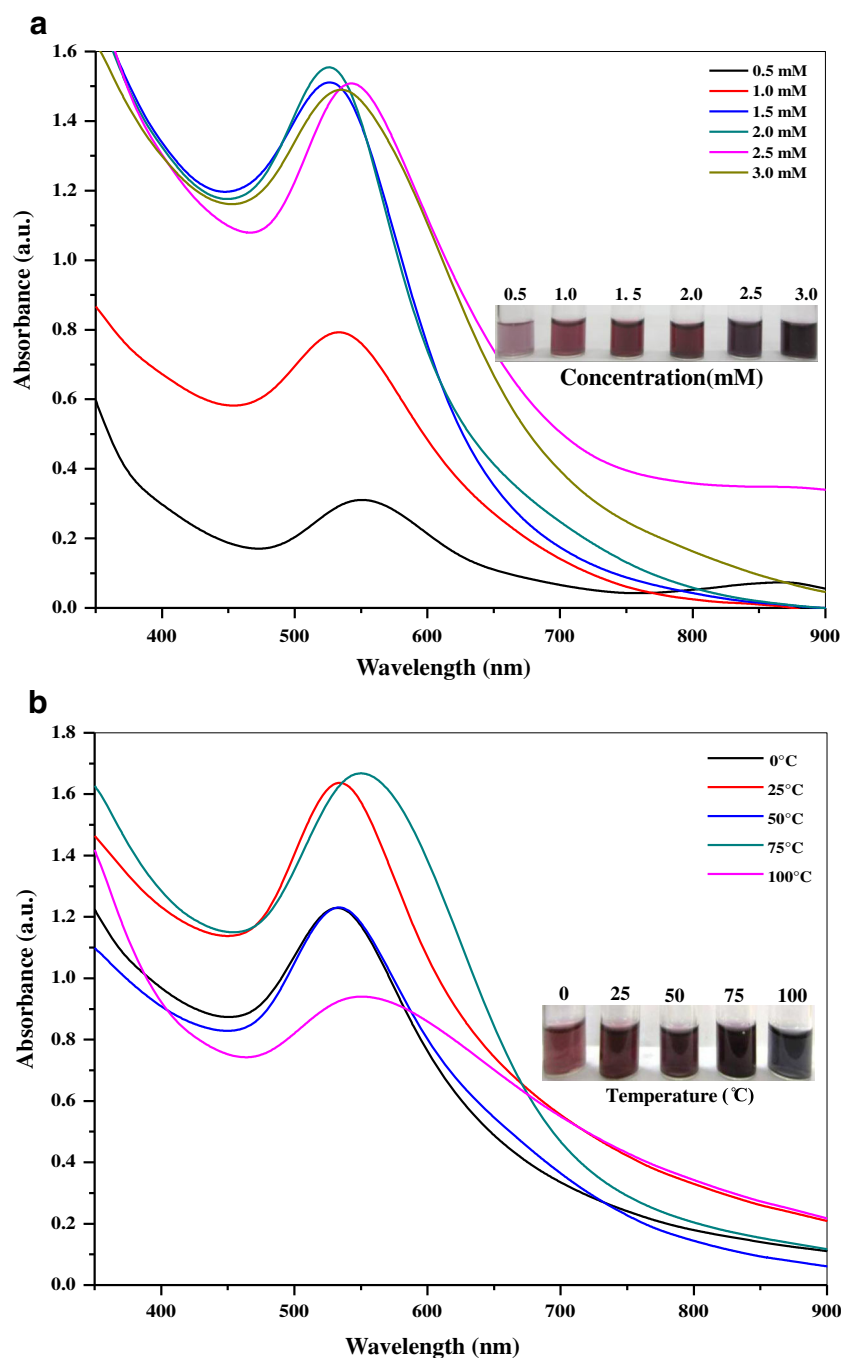
where d (nm) is the size of AuNPs, A_{spr} and A_{450} are absorbencies of QC-AuNPs at 525 nm and at 450 nm. The B_1 represents the inverse of slope (m; 3.55) of theoretical data. The B_2 is related to the B_0/m (3.11) where B_0 is the intercept. Based on these calculations, we found that the SPR peak of QC-AuNPs at 525 nm shows the particle size to be ~11.89 nm.

The hydrodynamic diameter and morphology of QC-AuNPs were characterized by DLS and TEM (Fig. 5a and e). As shown in Figs. 5a and e, the DLS data is well agreed with TEM and the average size of QC-AuNPs is found to be ~15 nm. These results suggest that the QC-AuNPs are well dispersed in solutions with an average diameter ~15 nm, which allows to use them as colorimetric probes for sensing of analytes. Since, the SPR peak of AuNPs at <530 nm exhibits <20 nm diameter with visible color as red.

QC-AuNPs as a smart nanoprobe for arginine, histidine and lysine

In order to investigate the smart nanoprobe ability of novel QC-AuNPs, different amino acids solutions (Arg, His, Lys, aspartic acid, cysteine, glutamic acid, methionine, phenyl alanine, serine, threonine and tyrosine, 1.0 mM, 100 μL) were added separately into 4.02 μM of QC-AuNPs solution at PBS buffer pH 5 and their UV-visible absorption spectra and color changes were measured. As shown in Fig. 2a, the

Fig. 1 **a** UV-visible absorption spectra of AuNPs by using quercetin as reducing and as capping agent at different concentrations 0.5–3.0 mM. **b** UV-visible absorption spectra of AuNPs by using QC (2.0 mM) as reducing and as capping agent at different reaction temperatures from 0 to 100 °C. Inset images are the corresponding photograph of QC-AuNPs



solutions containing Arg, His and Lys have shown distinct UV-visible spectral changes and changed the color from red to blue for three amino acids. The results obtained clearly indicate that except Arg, His and Lys no other amino acids exhibited any distinct color change. Importantly, UV-visible spectra also showed no existence of peaks at around 702, 693 and 745 nm in the other tested amino acids except Arg, His, and Lys, respectively. Supporting Information of Fig. S3 shows the selectivity of QC-AuNPs for colorimetric sensing of three amino acids.

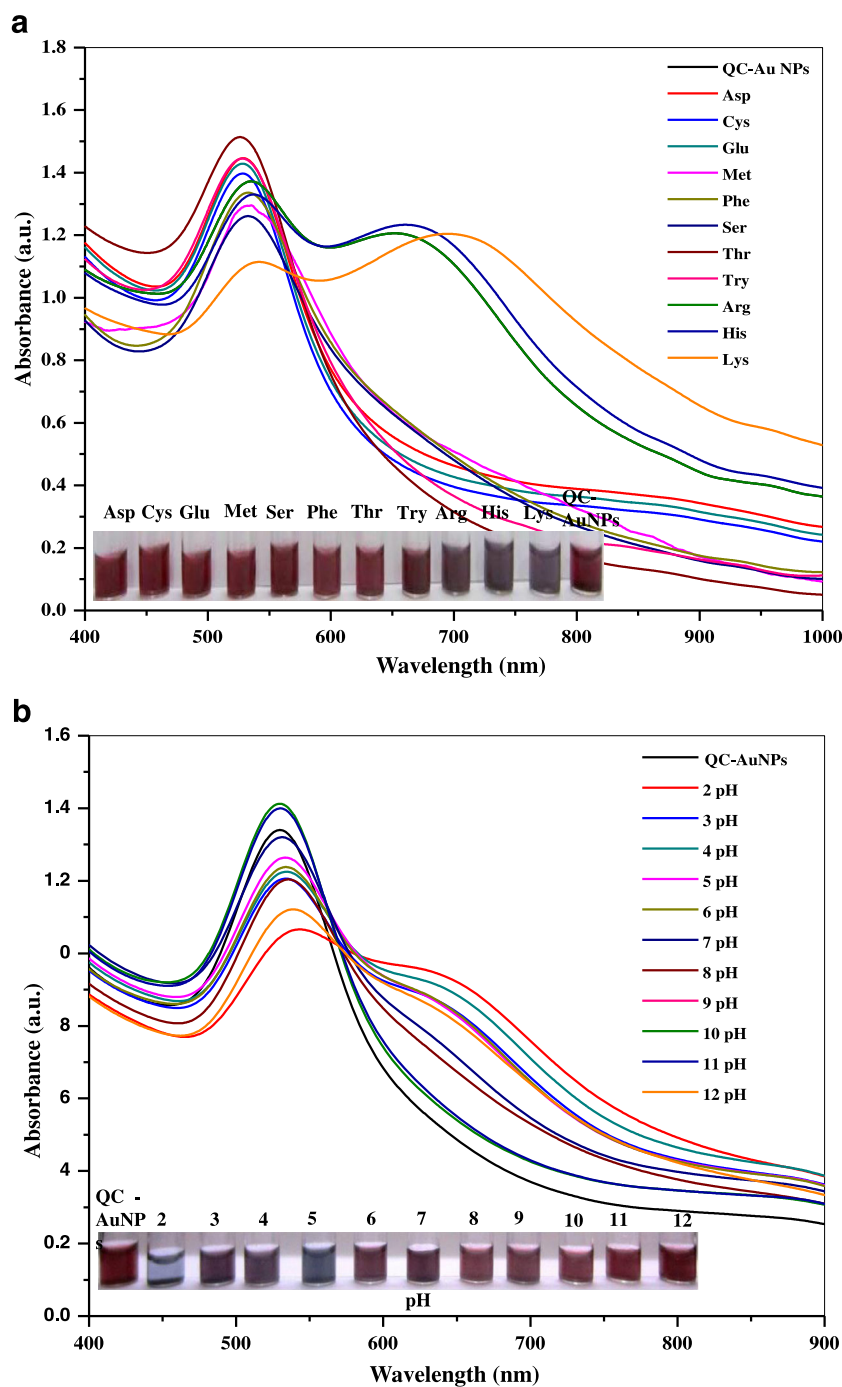
Effect of pH

We also studied the effect of buffers on QC-AuNPs molecular sensing ability for three amino acids by using different buffers such as PBS, Tris HCl and ammonium acetate. As shown in Supporting Information of Figs. S4–5, the absorbance ratios of (A_{702}/A_{525} , A_{693}/A_{525} and A_{745}/A_{525} for Arg, His and Lys) QC-AuNPs with three amino acids are higher at PBS buffer than that of Tris HCl and ammonium acetate as buffers. Therefore, we selected PBS as buffer media for the recognition of three amino

acids by using QC-AuNPs as a colorimetric probe. Furthermore, we also studied the effect of PBS buffer pH in the range of 2.0–12.0 for three amino acids. As shown in Fig. 2b and Supporting Information of Fig. S4, the color and absorbance ratios of QC-AuNPs are changed upon addition of three amino acids at PBS buffer pH range from 2.0 to 7.0. At lower pH values ($\text{pH} < 4$), the metallic NPs underwent self aggregation by the surface charge neutralization [28]. At the same time, the intensities ratios of (A_{702}/A_{525} , A_{693}/A_{525} and A_{745}/A_{525} for Arg, His and Lys) are higher at PBS buffer pH 5.0. We also believe that at this pH, the

aggregation of QC-AuNPs was greatly induced by target analytes through electrostatic interactions. Since, the pK_a of QC is ~ 5.0 [29, 30], and so at pH 5 and above most of the phenolic -OH groups will get negative charge (phenoxide ion). Meanwhile, three amino acids (Arg, $\text{pI} = 10.76$; His $\text{pI} = 7.59$, pI ; and Lys, $\text{pI} = 9.74$) will get positive charge ($\text{pH} < \text{pI}$), resulting strong electrostatic interactions between QC-AuNPs and amino acids. As a result, the original SPR band of QC-AuNPs at 525 nm decreases with the emergence of new SPR absorption bands at 702, 693 and 745 nm for Arg, His and Lys, respectively.

Fig. 2 **a** UV-visible absorption spectra of QC-AuNPs in the presence of different amino acids (aspartic acid, cysteine, glutamic acid, methionine, phenyl alanine, serine, threonine and tyrosine; 1.0 mM) at PBS buffer pH 5.0. **b** UV-visible absorption spectra of QC-AuNPs in the presence of Arg (1.0 mM) at various PBS buffer pH from 2.0 to 12.0. Photographic images of QC-AuNPs in the presence of Arg at various PBS buffer pH from 2.0 to 12.0



Moreover, obvious color change of QC-AuNPs solution from claret-red to blue could be observed by bare eyes as displayed in the inset of Fig. 2b and Supporting Information of Fig. S4. Therefore, pH 5.0 was chosen for QC-AuNPs-based colorimetric assays of three amino acids.

Colorimetric assay of three amino acids (Arg, His and Lys)

To test the analytical performance of QC-AuNPs, various concentrations of three amino acids were added into

individual QC-AuNPs solutions containing PBS buffer at pH 5.0. The changes of QC-AuNPs dispersions both in terms of the color and the absorbance spectra are recorded and shown in Figs. 3 and 4a. These results indicate that linear correlation existed between intensity ratios (A_{702}/A_{525} , A_{693}/A_{525} and A_{745}/A_{525} for Arg, His and Lys) and the logarithm of the Arg, His and Lys, concentrations over the range of 1.0 and 1,250 μM with correlation coefficients (R^2) 0.983, 0.989, and 0.987, respectively. The absorbance ratios (A_{702}/A_{525} , A_{693}/A_{525} and A_{745}/A_{525})

Fig. 3 UV-visible absorption spectra of QC-AuNPs in the presence of different concentrations of **a** Arg (2.5 – 1,250 μM) and **b** His (1.0 – 1,000 μM) at PBS buffer pH 5.0. Inset images are the corresponding photographs of QC-AuNPs color

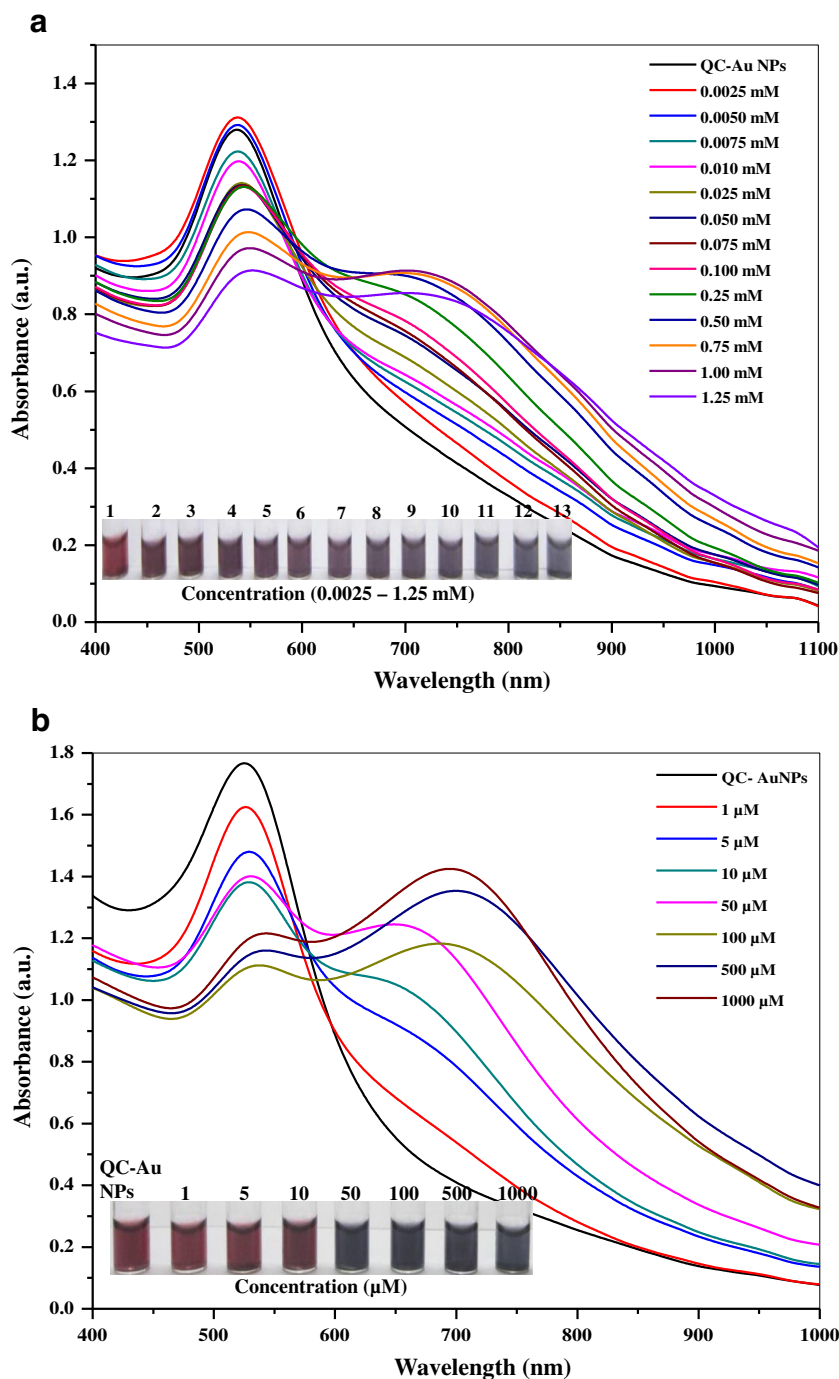
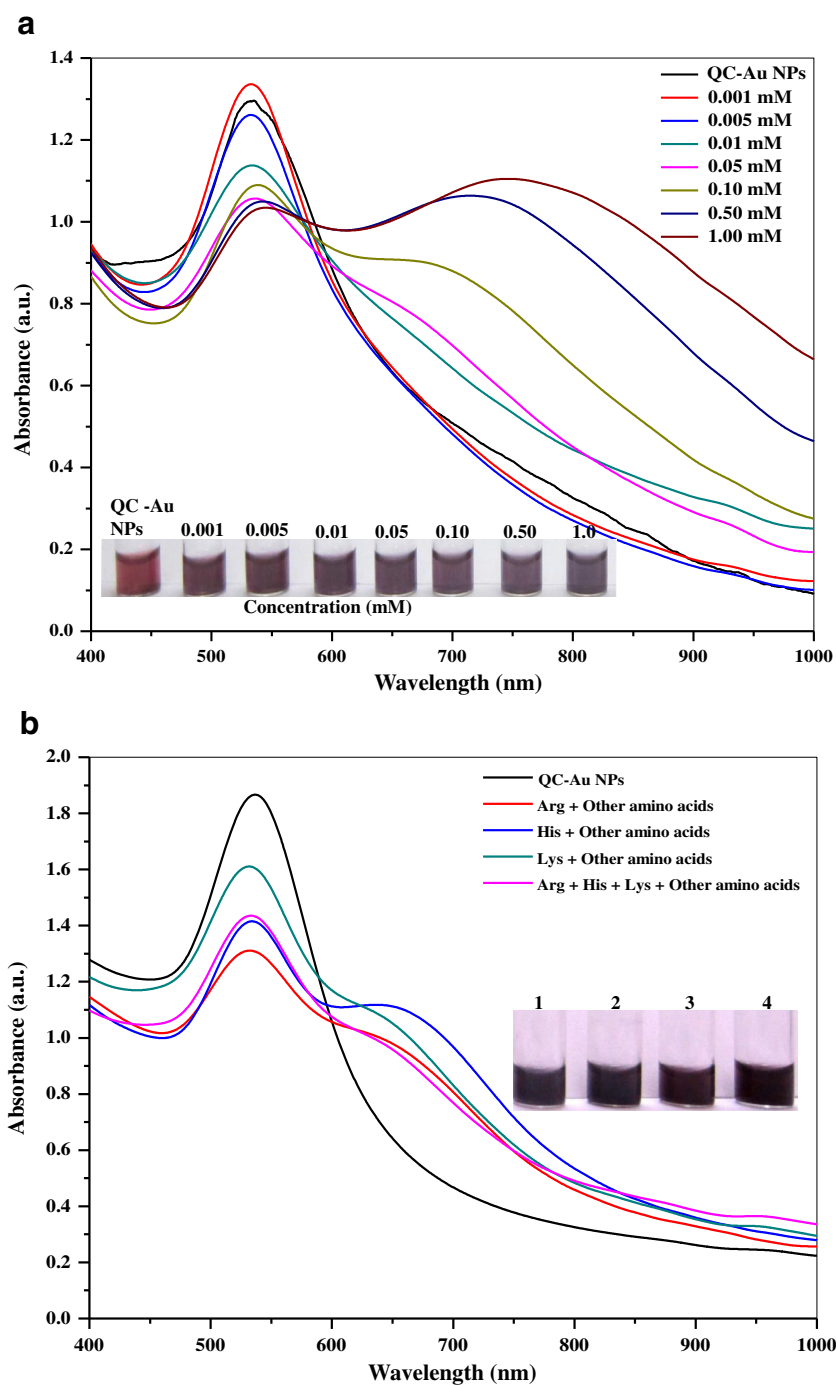


Fig. 4 a UV-visible absorption spectra of QC-AuNPs in the presence of different concentrations of Lys (1.0–1,000 μ M) at PBS buffer pH 5.0. **b** UV-visible absorption spectra of QC-AuNPs aggregated Arg, His and Lys (1.0 mM) in the presence of other amino acids (1.0 mM) at PBS buffer pH 5.0. Inset images are the corresponding photographs of QC-AuNPs color



are increased with increasing concentration of three amino acids concentrations in the system and showed a linear relationship for target analytes in the 2.5–1,250 μ M, 1–1,000 μ M and 1–1,000 μ M for Arg, His and Lys, respectively. As a result, limits of detections were found to be 0.04, 0.03, 0.02 μ M for Arg, His and Lys, respectively. Supporting Information of Fig. S6 show a linear correlation was observed between the ratios of absorbance (A_{702}/A_{525} , A_{693}/A_{525} and A_{745}/A_{525}) versus logarithm of three amino acids concentration (μ M).

In order to know the hydrodynamic diameter and morphology feature of QC-AuNPs before and after aggregation induced by target analytes, we studied DLS and TEM for the estimation of sizes and morphologies of QC-AuNPs. As shown in Fig. 5, as-prepared QC-AuNPs are well monodisperse with an average hydrodynamic diameter \sim 15 nm (Fig. 5a and e). However, after addition of Arg, His, and Lys into QC-AuNPs, the hydrodynamic diameter of QC-AuNPs are drastically increased to 165.4, 80.4 and 115.3 nm, which confirms that QC-AuNPs aggregation induced by Arg, His

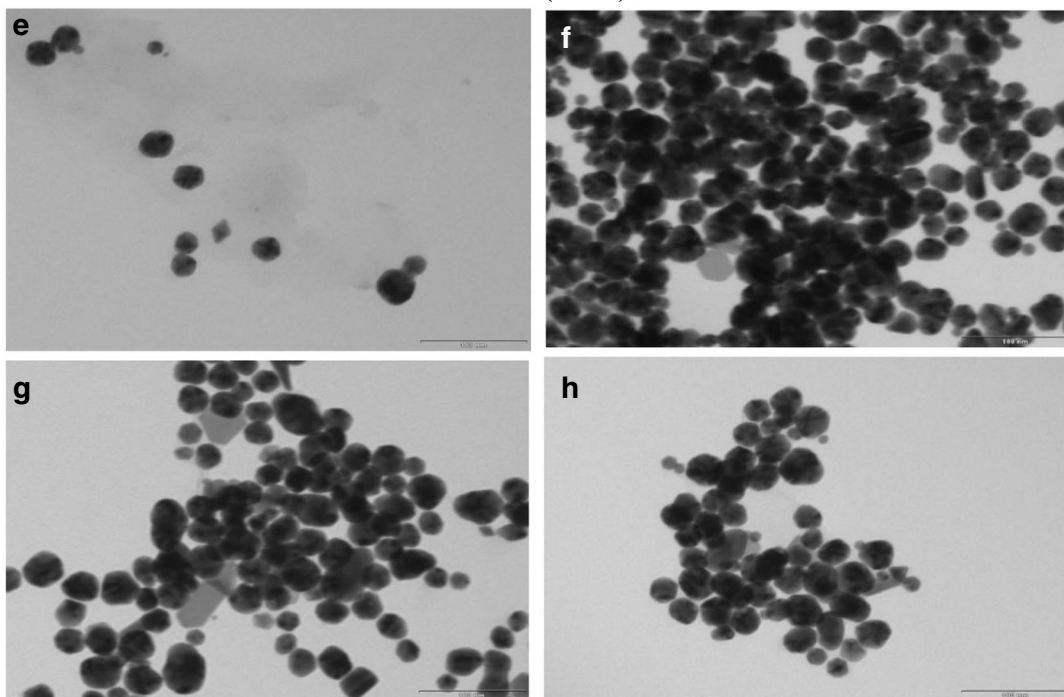
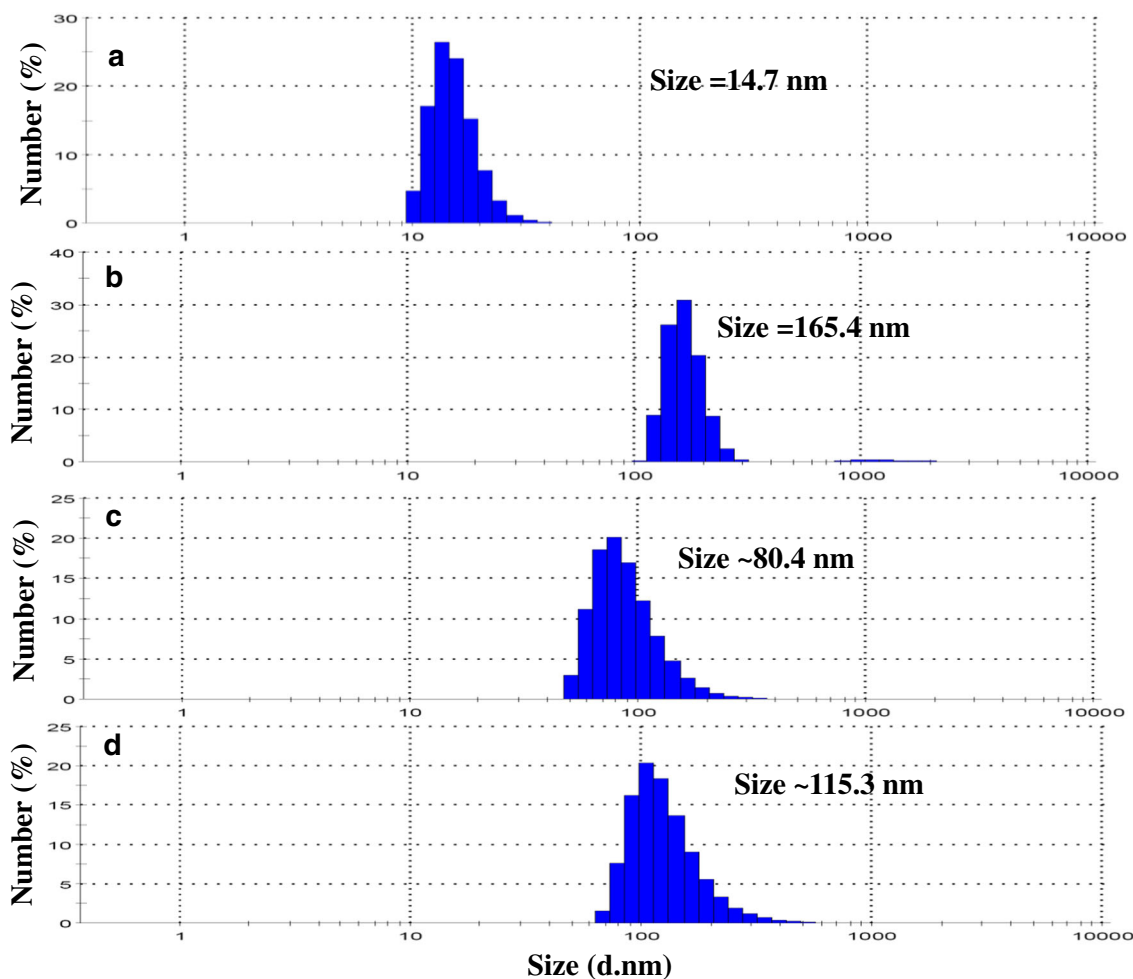


Fig. 5 DLS data of **a** QC-AuNPs and their induced aggregation with **b** Arg, **c** His, and **d** Lys. TEM images of **e** QC-AuNPs and their induced aggregations with **f** Arg, **g** His, and **h** Lys, respectively. TEM images are measured at 100 nm scale bar for all samples

and Lys, respectively (Fig. 5b–d). Figure 5e–h shows the TEM images of QC-AuNPs and their aggregation induced by Arg, His and Lys. These results indicate that the morphology of QC-AuNPs is completely changed due to their aggregations induced by three amino acids. As can be seen in Fig. 5e–h, the QC-AuNPs polydispersity was largely increased with their aggregation induced by Arg, His, and Lys, respectively. As a result, QC-AuNPs have an average size of ~15 nm, while their induced aggregated particles sizes were increased to 165.4, 80.4, and 115.3 nm for Arg, His and Lys, respectively. These results strongly suggest that the hydrodynamic diameter and particle size of QC-AuNPs were greatly increased due to their aggregation induced by three amino acids. It can also be observed that the hydrodynamic size of QC-AuNPs is comparatively large in DLS data, which is due to water absorption on electrostatic stabilized AuNPs. As can be seen from Fig. 5, the hydrodynamic diameters of QC-AuNPs and their aggregation induced by three amino acids were estimated in the range of 80.4–165.4 nm, while the TEM images of the above AuNPs were shown in Fig. 5.

Interference studies

Interference studies were carried out in order to explore the specific detection of Arg, His and Lys in biological samples using QC-AuNPs as a colorimetric probe. The UV-visible

spectra of QC-AuNPs with three amino acids (Arg, His and Lys) independently were measured in the presence of other amino acids (aspartic acid, cysteine, glutamic acid, methionine, phenyl alanine, serine, threonine and tyrosine, 1.0 mM). As shown in Fig. 4b, no obvious interferences were noticed in the presence of other amino acids. In order to estimate more selectivity of QC-AuNPs among three amino acids, we studied the UV-visible spectrum of QC-AuNPs by the addition of three amino acids (1.0 mM) along with the other amino acids (1.0 mM). We observed that QC-AuNPs have shown greater selectivity for Arg, His and Lys than that of aspartic acid, cysteine, glutamic acid, methionine, phenyl alanine, serine, threonine and tyrosine. These results indicate that other amino acids did not interfere in the aggregation of QC-AuNPs induced by Arg, His, and Lys, respectively. Furthermore, the influence of some possibly coexisting foreign substances including inorganic ions (Mg^{2+} , Ca^{2+} , Al^{3+} , Na^+ , K^+ , Ba^{2+} , 0.1 mM) and organic compounds (glucose, urea, uracil, guanine, guanosine, adinine and inosine, 0.1 mM) were tested for the analysis of His, Arg and Lys. As shown in Supporting Information of Figs. S7–8, no changes in the UV-visible spectra of QC-AuNPs with inorganic species and organic molecules, and there is no red-shift in the SPR peak of QC-AuNPs, which confirms that QC-AuNPs remained stable as a red monodispersion. However, a red shift in the wavelength and a change in color were observed only by the addition of

Table 1 Linear range, limit of detection (LOD), correlation coefficients (R^2), precision and accuracy of the method for the analysis of amino acids and His spiked urine using QC-AuNPs

Analyte	Linear range (μM)	LOD (μM)	R^2	Known concentration (μM)	Intra-day			Inter-day		
					Found concentration (μM) ^a	Precision (%) ^b	Accuracy (%) ^c	Found concentration (μM) ^a	Precision (%) ^b	Accuracy (%) ^c
Arg	2.5–1,250	0.04	0.983	5.0	5.04±0.15	3.6	+0.8	5.06±0.08	1.6	+1.2
				15.0	14.96±0.12	4.2	−4.0	15.03±0.06	0.4	+2.0
				25.0	25.02±0.53	1.6	+2.0	25.12±0.19	0.7	+4.8
Lys	1.0–1,000	0.02	0.989	5.0	4.87±0.18	3.7	−2.6	5.27±0.11	2.1	+5.4
				15.0	15.05±0.19	1.2	+3.3	15.02±0.23	1.5	+1.3
				25.0	25.30±0.37	0.9	+1.2	24.67±0.22	0.9	−1.3
His	1.0–1,000	0.03	0.987	5.0	5.00±0.11	2.2	+0.0	5.10±0.11	1.8	+2.0
				15.0	15.03±0.15	1.0	+2.0	14.98±0.48	2.3	−1.3
				25.0	25.07±0.78	3.1	+3.0	25.65±0.35	1.0	+2.6
His spiked female urine	–	–	–	5.0	5.80±0.14	2.0	+16.0	6.18±0.17	2.4	+23.6
				15.0	15.79±0.24	1.5	+5.2	15.83±0.28	1.7	+5.4
				25.0	26.09±0.65	2.5	+4.3	26.21±0.92	3.5	+4.8
His spiked male urine	–	–	–	5.0	6.30±0.23	1.8	+26.0	6.32±0.16	2.2	+26.4
				15.0	15.82±0.18	1.2	+5.4	15.41±0.21	1.1	+2.7
				25.0	26.45±0.10	0.3	+9.9	26.41±0.33	1.2	+5.6

^a Mean ± standard deviation ($n=5$). ^b Precision was calculated (RSD, %) from standard deviation/mean×100

^c Accuracy was calculated from (found concentration−known concentration)/known concentration×100

Arg, His and Lys to QC-AuNPs solutions containing the above foreign species (inorganic species and organic molecules), which was accompanied by aggregation of QC-AuNPs. These results indicate that QC-AuNPs can be efficiently used as a selective colorimetric probe for detection of Arg, His and Lys.

Application of QC-AuNPs for analysis of His in urine samples

The analytical performance of present method was applied for detection of His in real biological samples. Urine samples were collected from the healthy volunteers (male and female), Department of Applied Chemistry, S. V. National Institute of Technology, Surat, Gujarat, India. Before validation of the present method, we studied the spectral and color changes of QC-AuNPs at different dilutions (0-fold to 60-fold) and at different volume ratios (5:1 to 1:5, v/v) of urine samples (female and male) and obtained data were shown in Supporting Information of Figs. S9–11. It can be observed that the color of QC-AuNPs were drastically changed by the addition of the diluted urine samples (0-fold to 45-fold), resulting a red-shift in the SPR band. In contrast, while the addition of QC-AuNPs to the 50-fold of urine samples does not lead to the obvious change in either the color or the SPR band, as compared with those dilutions. Based on these results, we carried out the validation of the present method for the quantification of His in urine samples at 50-fold dilution. The diluted urine samples were spiked with known

concentration of His and then added independently into QC-AuNPs. Intra-day precision and accuracy were determined by repeated analysis of three amino acids from aqueous samples and of His from urine samples in one day ($n=5$), while the inter-day precision and accuracy of the method was performed in different time intervals in one day (Supporting Information of Fig. S12). Accuracy and precision for intra- and inter-day urine samples of three amino acids were tested at three concentration levels (5.0, 15, and 25 μM) and the data are presented in Table 1. Intra- and inter-day accuracy and precision of the method was found to be -1.3 – 3.0 % and 1.0 – 3.1 % for His and -4.0 – 4.8 %, 0.4 – 4.2 % for Arg and -2.6 – 5.4 % and 0.9 – 3.7 % for Lys, respectively. The intra assay precision was <4.2 % RSD and the inter assay precision was <2.3 % RSD for three amino acids. It can be observed that the % recoveries for His in the urine samples were higher than 100, this is due to the presence of His in human urine [31]. These results indicate that the present method shows good reproducibility and repeatability for the analysis of three amino acids from biological samples with higher sensitivity, simple sample pre-treatment, faster analysis, and in particular visual identification.

Table 2 shows the comparison of the present method with the other analytical techniques such as thin layer chromatography [32], HPLC [33], gas chromatography-mass spectrometry (GC-MS) [34] and capillary electrophoresis [35] for the analysis of amino acids. The present method shows good agreement with HPLC, GC-MS and CE techniques. The LODs of the present method are close to CE and GC-MS

Table 2 Comparison of the present method with the other analytical techniques in the literature for the analysis of amino acids

Name of nano probes	Analytes	Linear range	LOD	Technique	Reference
Carboxymethyl cellulose-AuNPs	Cysteine	10.0–100.0 ^a	–	UV-visible	13
ssDNA-AuNPs	Cysteine	0.1–5.0 ^a	0.1 ^a	UV-visible	14
Sulfonato-calix[4]arene thiol-AuNPs	Lys	1.0–100 ^a	1.0 ^b	UV-visible	15
	Arg	4.0–100 ^a	4.0 ^b		
	His	2.0–100 ^a	2.0 ^b		
Poly(9,9-bis(4 ϕ -sulfonatobutyl) fluorene-co-alt-1,4-phenylene) sodium salt- AuNPs	Cysteine	0.05–4.0 ^a	25.0 ^c	UV-visible and fluorescence	17
Thermoresponsive copolymer-AuNPs	Cysteine	1.0–6.0 ^a	–	UV-visible	19
Glutathione-AuNPs	Cysteine	–	<3.0 ^c	UV-visible and fluorescence	21
	His	2.0–30 ^a	0.4 ^a	UV-visible	30
–	22 amino acids	–	0.01–1.0 ^d	Thin layer chromatography	31
–	26 amino acid	2.5–100 ^c	–	HPLC	32
–	D-amino acids	–	3.2–446 ^c	GC-MS	33
–	Tryptophan	1.7–3.7 ^a	0.15 ^c	Capillary electrophoresis	34
	Tyrosine	6.6–13.7 ^a	50 ^c	Capillary electrophoresis	
QC-AuNPs	Arg	2.5–1250 ^a	40 ^c	UV-visible	Present method
	His	1.0–1000 ^a	30 ^c		
	Lys	1.0–1000 ^a	20 ^c		

^a μM , ^b mM , ^c nM , ^d μg and ^e $\text{pmol} \cdot \mu\text{L}^{-1}$

techniques and lower than the HPLC. However, this method was successfully applied to determine amino acids in biological samples with very short time and with minimized sample preparation.

Conclusions

In this report, we introduced a novel reagent for preparation and functionalization of AuNPs for selective colorimetric sensing of three amino acids (Arg, His, and Lys) in biological samples. We studied various influencing parameters such as effect of reagent, temperature and reaction time for the preparation of controlled size AuNPs. The QC-AuNPs acted as effective colorimetric probe at pH 5.0 for on-site and real-time detection of three amino acids in urine samples. Three amino acids showed high affinity to induce aggregation of QC-AuNPs thereby resulting in change in color from red to blue. This study also shows that QC-AuNPs has a higher affinity for Arg, His and Lys compared to aspartic acid, cysteine, glutamic acid, methionine, phenyl alanine, serine, threonine and tyrosine. Furthermore, the preparation and functionalization of AuNPs with QC is simple, and operated under sample-friendly conditions. We anticipate that the QC-AuNPs as nonoprobes will open new ways for amino acids analysis and their investigations in biocomplex samples.

Acknowledgements This research was supported by the DST, India under DST-Inspire Fellowship Ph.D. Programme. The authors would like to thank Prof. Murthy, and Mr. Chetan Patel for the help with the DLS measurements. We also thank Department of Science and Technology for providing Maya Pro 2,000 spectrophotometer under the Fast-Track Young Scientist Scheme (2011–2014).

References

1. Wolfbies OS (2013) Probes, sensors, and labels: Why is real progress slow? *Angew Chem Int Ed* 52:9864–9865
2. Vilela D, González MC, Escarpa A (2012) Sensing colorimetric approaches based on gold and silver nanoparticles aggregation: chemical creativity behind the assay. A review. *Anal Chim Acta* 751:24–43
3. Saha K, Agasti SS, Kim C, Li X, Rotello VM (2012) Gold nanoparticles in chemical and biological sensing. *Chem Rev* 112:2739–2779
4. Baptista P, Pereira E, Eaton P, Doria G, Miranda A, Gomes I, Quaresma P, Franco R (2008) Gold nanoparticles for the development of clinical diagnosis methods. *Anal Bioanal Chem* 391:943–950
5. Wang Z, Ma L (2009) Gold nanoparticle probes. *Coord Chem Rev* 253:1607–1618
6. Eustis S, El-Sayed MA (2006) Why gold nanoparticles are more precious than pretty gold: noble metal surface plasmon resonance and its enhancement of the radiative and nonradiative properties of nanocrystals of different shapes. *Chem Soc Rev* 35:209–217
7. Turkevich J, Stevenson PC, Hillier J (1951) A study of the nucleation and growth processes in the synthesis of colloidal gold. *Discuss Faraday Soc* 11:55–75
8. Kappi FA, Tsogas GZ, Giokas DL, Christodouleas DC, Vlessidis AG (2014) Colorimetric and visual read-out determination of cyanuric acid exploiting the interaction between melamine and silver nanoparticles. *Microchim Acta* 181:623–629
9. Gazit V, Ben-Abraham R, Coleman R, Weizman A, Katz Y (2004) Cysteine-induced hypoglycemic brain damage: an alternative mechanism to excitotoxicity. *Amino Acids* 26:163–168
10. Lee IL, Sung YM, Wu CH, Wu SP (2014) Colorimetric sensing of iodide based on triazole-acetamide functionalized gold nanoparticles. *Microchim Acta* 181:573–579
11. Chansuvarn W, Imyim A (2012) Visual and colorimetric detection of mercury(II) ion using gold nanoparticles stabilized with a dithia-diaza ligand. *Microchim Acta* 176:57–64
12. Haghazari N, Alizadeh A, Karami C, Hamidi Z (2013) Simple optical determination of silver ion in aqueous solutions using benzo crown-ether modified gold nanoparticles. *Microchim Acta* 180:287–294
13. Wei X, Qi L, Tan J, Liu R, Wang F (2010) A colorimetric sensor for determination of cysteine by carboxymethyl cellulose-functionalized gold nanoparticles. *Anal Chim Acta* 671:80–84
14. Chen Z, Luo S, Liu C, Cai Q (2009) Simple and sensitive colorimetric detection of cysteine based on ssDNA-stabilized gold nanoparticles. *Anal Bioanal Chem* 395:489–494
15. Patel G, Menon S (2009) Recognition of lysine, arginine and histidine by novel p-sulfonatocalix[4]arene thiol functionalized gold nanoparticles in aqueous solution. *Chem Commun* 45:3563–3565
16. Chang CW, Tseng WL (2010) Gold nanoparticle extraction followed by capillary electrophoresis to determine the total, free, and protein-bound amino thiols in plasma. *Anal Chem* 82:2696–2702
17. Shang L, Qin CJ, Wang T, Wang M, Wang LX, Dong SJ (2007) Fluorescent conjugated polymer-stabilized gold nanoparticles for sensitive and selective detection of cysteine. *J Phys Chem C* 111:13414–13417
18. Zhong ZY, Patskovskyy S, Bouvrette P, Luong JHT, Gedanken A (2004) The surface chemistry of Au colloids and their interactions with functional amino acids. *J Phys Chem B* 108:4046–4052
19. Okubo K, Shimada T, Shimizu T, Uehara N (2007) Simple and selective sensing of cysteine using gold nanoparticles conjugated with a thermoresponsive copolymer having carboxyl groups. *Anal Sci* 23:85–90
20. Vemula PK, Aslam U, Mallia VA, George J (2007) In situ synthesis of gold nanoparticles using molecular gels and liquid crystals from vitamin-c amphiphiles. *Chem Mater* 19:138–140
21. Yuan X, Tay Y, Dou X, Luo Z, Leong DT, Xie J (2013) Glutathione-protected silver nanoclusters as cysteine-selective fluorometric and colorimetric probe. *Anal Chem* 85:1913–1919
22. Liu D, Chen W, Wei J, Li X, Wang Z, Jiang X (2012) A highly sensitive, dual-readout assay based on gold nanoparticles for organophosphorus and carbamate pesticides. *Anal Chem* 84:4185–4191
23. Zhu K, Zhang Y, He S, Chen W, Shen J, Wang Z, Jiang X (2012) Quantification of proteins by functionalized gold nanoparticles using click chemistry. *Anal Chem* 84:4267–4270
24. Cao Q, Zhao H, He Y, Li X, Zeng L, Ding N, Wang J, Yang J, Wang G (2010) Hydrogen-bonding-induced colorimetric detection of melamine by nonaggregation-based Au-NPs as a probe. *Biosens Bioelectron* 25:2680–2685
25. Yoosaf K, Ipe BI, Suresh CH, Thomas KG (2007) In situ synthesis of metal nanoparticles and selective naked-eye detection of lead ions from aqueous media. *J Phys Chem C* 111:12839–12847
26. Miguel-García I, Berenguer-Murcia Á, García T, Cazorla-Amorós D (2012) Effect of the aging time of PVP coated palladium nanoparticles colloidal suspensions on their catalytic activity in the preferential oxidation of CO. *Catal Today* 187:2–9
27. Haiss W, Thanh NTK, Aveyard J, Fernig DG (2007) Determination of size and concentration of gold nanoparticles from UV-vis spectra. *Anal Chem* 79:4215–4221

28. Basu S, Ghosh SK, Kundu S, Panigrahi S, Praharaj S, Pande S, Jana S, Pal T (2007) Biomolecule induced nanoparticle aggregation: effect of particle size on interparticle coupling. *J Colloid Interface Sci* 313: 724–734
29. Ramešová S, Sokolová R, Degano I, Bulíčková J, Žabka J, Gál M (2012) On the stability of the bioactive flavonoids quercetin and luteolin under oxygen-free conditions. *Anal Bioanal Chem* 402: 975–982
30. Zenkevich IG, Guschina SV (2010) Determination of dissociation constants of species oxidizable in aqueous solution by air oxygen on an example of quercetin. *J Anal Chem* 65:371–375
31. Sun SK, Tu KX, Yan XP (2012) An indicator-displacement assay for naked-eye detection and quantification of histidine in human urine. *Analyst* 137:2124–2128
32. Sinhababu A (2013) Modified ninhydrin reagent for the detection of amino acids on TLC plates. *J Appl Nat Sci* 5:125–127
33. Sharma G, Attri SV, Behra B, Bhisikar S, Kumar P, Tajeja M, Sharda S, Singhi P, Singhi S (2014) Analysis of 26 amino acids in human plasma by HPLC using AQC as derivatizing agent and its application in metabolic laboratory. *Amino Acids* 46:1253–1263
34. Waldhier MC, Dettmer K, Gruber MA, Oefner PJ (2010) Comparison of derivatization and chromatographic methods for GC-MS analysis of amino acid enantiomers in physiological samples. *J Chromatogr B* 878:1103–1112
35. Bayle C, Siri N, Poinot V, Treilhou M, Causse E, Couderc F (2003) Analysis of tryptophan and tyrosine in cerebrospinal fluid by capillary electrophoresis and “ball lens” UV-pulsed laser-induced fluorescence detection. *J Chromatogr A* 1013:123–130